E-proceedings of the 38th IAHR World Congress
September 1-6, 2019, Panama City, Panama
doi:10.3850/38WC092019-0685

ANALYSIS OF FLOWS IN UNDULAR AND BREAKING HYDRAULIC JUMPS BY NON-HYDROSTATIC QUASI THREE-DIMENSIONAL MODEL CONSIDERING FLOW EQUATIONS ON BOUNDARY SURFACES (Q3D-FEBS)

YOSHIHARU TAKEMURA [1] & SHOJI FUKUOKA [2]

[1] Research and Development Initiative, Chuo University, Tokyo, Japan,
takemura@tamacc.chuo-u.ac.jp

[2] Research and Development Initiative, Chuo University, Tokyo, Japan,
sfuku@tamacc.chuo-u.ac.jp

ABSTRACT

The flow structure and the energy dissipation rate are greatly different between an undular jump and a breaking jump. A depth-integral model that can calculate both undular and breaking jumps is required for the design of hydraulic structures in rivers. This paper proposes a new non-hydrostatic quasi three-dimensional model (Q3D-FEBS) that introduces the flow equations on boundary surfaces (a free surface and a bottom surface). Calculation results of Q3D-FEBS well explain water surface profiles and velocity distributions of the previous experiments of undular and breaking jumps. In addition, based on a numerical experiment, it is shown that Q3D-FEBS can calculate the transitional process from an undular jump to a breaking jump by analyzing the flow separation at the water surface using the flow equations on boundary surfaces.

Keywords: Undular jump; breaking jump; non-hydrostatic pressure; depth-integral model; Q3D-FEBS

1 INTRODUCTION

A hydraulic jump occurs in various forms depending mainly on the Froude number (Fr). The forms can be divided roughly into following two types. For 1.7 > Fr > 1, a wavy water surface is formed downstream of a hydraulic jump and the jump called an undular jump. For Fr > 1.7, a surface roller develops just below the water surface of a hydraulic jump and the jump called a breaking jump. Since the flow structure and the energy dissipation rate of the undular and breaking jumps are greatly different from each other, it is necessary to accurately predict the forms of the jump under given hydraulic conditions. 3D-RANS and MPS are effective method for such problems. However, more efficient method based on a depth-integral model is needed for large-scale flows varying in time and space such as flows around hydraulic structures in rivers during floods. Although many researchers have proposed depth-integral models for hydraulic jumps, there is no depth-integral model that can calculate both undular and breaking jumps including the transitional process between the jumps.

Most of the models for undular jumps have been developed based on the Boussinesq type equation that considers non-hydrostatic pressure due to the curvature of the water surface (e.g. Serre 1953, Iwasa 1955, Hosoda & Tada 1994 and Castro-Orgaz et al. 2015), and usually neglect the velocity distributions along vertical direction. In contrast, the models for breaking jumps have been developed based on the strip integral method that assumes velocity distributions within the jump using the wall jet theory or polynomials (Narayanan 1975, McCorquodale & Khalifa 1983, Tsubaki 1949 and Madsen & Svendsen 1983), and neglect non-hydrostatic pressure in many cases. In order to calculate both undular and breaking jumps in the framework of the depth-integral model, it is necessary to model the three-dimensional velocity and the non-hydrostatic pressure distributions in a generalized manner as much as possible.

This paper proposes a new non-hydrostatic quasi three-dimensional model (Q3D-FEBS) that introduces the flow equations on the boundary surfaces (free surfaces and bottom surfaces) and investigates the applicability of Q3D-FEBS to the calculation of undular and breaking jumps including the transitional process between the jumps by using the previous experiments and a numerical simulation.

2 GORVERNING EQUATIONS OF Q3D-FEBS

The definition sketch of Q3D-FEBS (Ohno et al, 2018) is shown in Figure 1. We define the bottom surface z_b slightly above the bed surface z_0. A vertical coordinate is given as $\eta = (z_s - z)/h$ and approximates vertical distributions of the horizontal velocities by third-order polynomials.

$$u_i = \Delta u_i(12\eta^3 - 12\eta^2 + 1) + \delta u_i(-4\eta^3 + 3\eta^2) + U_i \quad [1]$$

Where, $i = 1, 2$ ($x_1 = x$, $x_2 = y$), u_i: velocity in i direction, U_i: depth-average velocity in i direction, u_{si}: water surface velocity in i direction, u_{bi}: bottom surface velocity in i direction, $\Delta u_i = u_{si} - U_i$, $\delta u_i = u_{si} - u_{bi}$, z_s: water level, h: water depth. The boundary conditions used in the derivation of Eq. [1] are as follows.

$$u_i = u_{si}, \quad \partial u_i/\partial z = 0 \quad at \quad \eta = 0\ (z = z_s) \tag{2}$$

$$u_i = u_{bi} \quad at \quad \eta = 1\ (z = z_b) \tag{3}$$

$$\int_0^1 u_i\, d\eta\ \left(= \frac{1}{h}\int_{z_b}^{z_s} u_i\, dz\right) = U_i \tag{4}$$

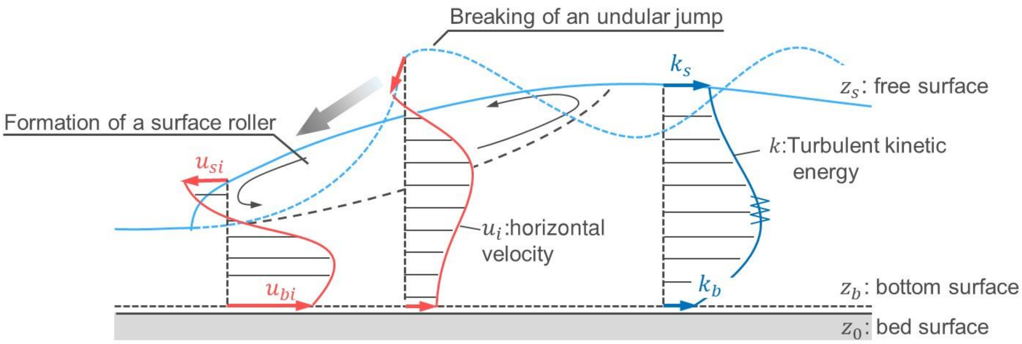

Figure 1. Definition sketch of Q3D-FEBS.

Q3D-FEBS solves the equations of motion on a free surface ($\eta = 0$) and a bottom surface ($\eta = 1$) in addition to the depth-integral flow equations shown by Eq. [5] and Eq. [6] to calculate the unknown quantities of Eq. [1].

$$\frac{\partial h}{\partial t} + \frac{\partial U_i h}{\partial x_i} = 0 \tag{5}$$

$$\frac{\partial U_i h}{\partial t} + \frac{\partial U_j U_i h}{\partial x_j} = -gh\frac{\partial z_s}{\partial x_i} - \frac{1}{\rho}\frac{\partial h\overline{p'}}{\partial x_i} - \frac{p'_b}{\rho}\frac{\partial z_b}{\partial x_i} - \frac{\partial h\overline{u'_i u'_j}}{\partial x_j} + \frac{\partial}{\partial x_j}\overline{\nu_t}h\left(\frac{\partial U_i}{\partial x_j} + \frac{\partial U_j}{\partial x_i}\right) - \hat{S}\frac{\hat{\tau}_{bi}}{\rho} \tag{6}$$

Where, ρ: density of water, $u'_i = u_i - U_i$, g: acceleration of gravity, p': non-hydrostatic pressure, ν_t: eddy viscosity, $\hat{\tau}_{bi}$: bottom shear stress in i direction, $\hat{S} = \sqrt{1 + (\partial z_b/\partial x_i)^2}$. Overbar "–" represents a depth-averaged value. Eq. [6] has the non-hydrostatic pressure terms and they are calculated from Eq. [7] derived from the depth-integral equation of motion in vertical direction.

$$\frac{p'_b}{\rho} = U_i h\frac{\partial W}{\partial x_i} + \hat{S}\frac{\hat{\tau}_{bz}}{\rho}, \frac{\overline{p'}}{\rho} = \frac{1}{2}\frac{p'_b}{\rho} + \frac{U_i h}{12}\frac{\partial(w_s - w_b)}{\partial x_i} \tag{7}$$

Where, W: depth-average velocity in vertical direction, w_s: water surface velocity in vertical direction, w_b: bottom surface velocity in vertical direction. W is obtained from Eq. [1] and the equation of continuity.

$$W = \frac{1}{2}\frac{\partial(z_s + z_b)}{\partial t} + \frac{1}{2}U_i\frac{\partial(z_s + z_b)}{\partial x_i} + \frac{1}{h}\frac{\partial}{\partial x_i}h^2\left(\frac{\delta u_i}{20} + \frac{\Delta u_i}{10}\right) \tag{8}$$

w_s and w_b are given from the kinematic boundary conditions at a water surface and a bottom surface.

$$w_s = \frac{\partial z_s}{\partial t} + u_{si}\frac{\partial z_s}{\partial x_i}, \quad w_b = \frac{\partial z_b}{\partial t} + u_{bi}\frac{\partial z_b}{\partial x_i} \tag{9}$$

Eq. [10] and Eq. [11] are the equations of motion on a water surface ($\eta = 0$) and a bottom surface ($\eta = 1$).

$$\frac{\partial u_{si}}{\partial t} + u_{sj}\frac{\partial u_{si}}{\partial x_j} = -g\frac{\partial z_s}{\partial x_i} + \frac{1}{\rho}\frac{\partial p'}{\partial z}\bigg|_s\frac{\partial z_s}{\partial x_i} + \frac{\nu_{ts}}{\rho}\frac{\partial^2 u_i}{\partial z^2}\bigg|_s \tag{10}$$

$$\frac{\partial u_{bi}}{\partial t} + u_{bj}\frac{\partial u_{bi}}{\partial x_j} = -g\frac{\partial z_s}{\partial x_i} - \frac{1}{\rho}\frac{\partial p'_b}{\partial x_i} + \frac{1}{\rho}\frac{\partial p'}{\partial z}\bigg|_b\frac{\partial z_b}{\partial x_i} + \frac{\partial}{\partial x_j}\nu_{tb}\left(\frac{\partial u_{bi}}{\partial x_j} + \frac{\partial u_{bj}}{\partial x_i}\right) + \frac{\hat{S}}{\rho}\frac{\hat{\tau}_{bi} - \hat{\tau}_{0i}}{\delta z_b} \tag{11}$$

Where, $\hat{\tau}_{0i}$: bed shear stress in i direction, $\delta z_b = c_{zb}h$, c_{zb} = 0.03. The shear stress and pressure at a water surface are assumed 0. The gradient of the non-hydrostatic pressure in vertical direction at a water surface and a bottom surface are calculated from Eq. [12] derived from the equations of motion in the vertical direction on a water surface and a bottom surface.

$$\frac{1}{\rho}\frac{\partial p'}{\partial z}\bigg|_s = -u_{si}\frac{\partial w_s}{\partial x_i}, \quad \frac{1}{\rho}\frac{\partial p'}{\partial z}\bigg|_b = -u_{bi}\frac{\partial w_b}{\partial x_i} \qquad [12]$$

The bottom shear stress and the bed shear stress are evaluated by Eq. [13] and Eq. [14], respectively.

$$\hat{\tau}_{0i} = \rho c_b^2 u_{bi}|\boldsymbol{u_b}|, \ \ \hat{\tau}_{0z} = \rho c_b^2 w_b|\boldsymbol{u_b}| \qquad [13]$$

$$\hat{\tau}_{bi} = \nu_{tb}\frac{\partial u_i}{\partial z}\bigg|_b, \ \ \hat{\tau}_{bz} = \frac{\hat{\tau}_{0z}}{c_{zb}+1} \qquad [14]$$

$$c_b = \frac{C_0}{1-2C_0/\kappa}\sqrt{1+c_{zb}}, \quad C_0 = \sqrt{\frac{gn^2}{h^{1/3}}} \qquad [15]$$

Where, $\partial^2 u_i/\partial z^2|_s = (-24\Delta u_i + 6\delta u_i)/h^2$, $\partial u_i/\partial x|_s = (-12\Delta u_i + 6\delta u_i)/h$, n: Manning's roughness coefficient, κ = 0.41.

Q3D-FEBS introduces the one equation turbulence model shown in Eq. [16] and Eq. [17] to analyze the energy dissipation process due to a hydraulic jump. These equations are derived by approximating the vertical distribution of the turbulent kinetic energy with the third-order polynomial as in Eq. [1].

$$\frac{\partial K}{\partial t} + U_i\frac{\partial K}{\partial x_i} = -\frac{1}{h}\frac{\partial h\overline{u_i'k'}}{\partial x_i} + \frac{1}{h}\frac{\partial}{\partial x_i}\frac{h\overline{\nu_t}}{\sigma_k}\frac{\partial K}{\partial x_i} + \frac{\nu_{tb}}{\sigma_k}\frac{\partial^2 k}{\partial z^2}\bigg|_b + \overline{P_k} - c_d\frac{K^{3/2}}{l_d} \qquad [16]$$

$$\overline{P_k} = c_h\overline{\nu_t}\left[\frac{1}{2}\left(\frac{\partial U_i}{\partial x_j} + \frac{\partial U_j}{\partial x_i}\right)^2 + \frac{24}{5h^2}(4\Delta u_i^2 - 7\delta u_i\Delta u_i + \delta u_i^2)\right] \qquad [17]$$

$$\frac{\partial k_s}{\partial t} + u_{si}\frac{\partial k_s}{\partial x_i} = \frac{\partial}{\partial x_i}\frac{\nu_{ts}}{\sigma_k}\frac{\partial k_s}{\partial x_i} + \frac{\nu_{ts}}{\sigma_k}\frac{\partial^2 k}{\partial z}\bigg|_s - c_d\frac{k_s^{3/2}}{l_d} \qquad [18]$$

$$k_b = \left(\frac{\alpha}{c_l}\right)^2\frac{u_*^2}{1+c_{zb}} \qquad [19]$$

Where, K: depth-average turbulent kinetic energy, k_s: turbulent kinetic energy at a water surface, k_b: turbulent kinetic energy at a bottom surface, $\overline{P_k}$: depth-average production rate of turbulent kinetic energy,σ_k = 1.0, c_d = 0.08, $l_d = c_l h$, c_l=0.07, c_h=0.5. The eddy viscosities are given as $\overline{\nu_t} = l_d\sqrt{K}$, $\nu_{ts} = l_d\sqrt{\nu_{ts}}$, $\nu_{tb} = l_d\sqrt{\nu_{tb}}$.

3 Application to the previous experiments of undular and breaking jumps

Q3D-FEBS is applied to the previous experiments of an undular jump (Chanson 1993) and a breaking jump (Chacherea & Chanson 2010). The experimental conditions are shown in Table 1.

Table 1. Conditions of the previous experiments of an undular jump and a breaking jump.

	Forms of the jump	Channel length	Channel width	Channel slope	Rate of flow	Fr	Re	Aspect ratio
Chanson 1993.	Undular jump	20 m	0.25 m	1/225	4.96 10^{-3}m^3/s	1.27	2.1×10^4	8.7
Chacherea & Chanson 2010.	Breaking jump	3.2 m	0.5 m	Horizontal	44.6 10^{-3}m^3/s	3.1	8.9×10^4	11.0

In the undular jump experiment (Chanson 1993), the location of the jump was controlled between 9.5 m and 15 m from the upstream end of the channel. Water depths and pressure distributions were measured on the centerline of the channel using a pointer gauge and a Pitot tube. The calculation was performed under the same conditions as the experiment. In order to investigate the influences of a computational grid size Δx on the calculation results, Δx = 0.01 m($\Delta x/h_2 \cong$ 0.25, h_2 : downstream sequent depth) and Δx = 0.004 m($\Delta x/h_2 \cong$ 0.1) were used. Figure 2 shows the comparison of measured and calculated water depth profiles. The longitudinal distance and the water depths are normalized by the critical depth h_c, respectively. The calculation results tend to overestimate an attenuation of the waves seen in the measured data. The calculated water surface profile of Δx = 0.01 m indicated by a black solid line can explain the experimental data up to the first wave crest. On the other hand, the result of Δx = 0.004 m indicated by a red solid line can reproduce the measured data up to the second wave trough. Figure 3 shows the comparison of the vertical distributions of measured and calculated pressure intensity at the crest and trough of the first and second waves on the channel centerline. The distributions of the pressure intensity are normalized by the hydrostatic pressure intensity at a bottom surface and the black solid lines in Figure 3 indicate hydrostatic pressure distributions. As shown in ○ and ×, the pressure intensity of the undular jump is lower at the crest and higher at the trough compared to the hydrostatic pressure distributions. The pressure distributions calculated by Q3D-FEBS using Δx = 0.004 m are in good agreement with measured data, but the results using Δx = 0.01 m cannot explain the pressure distribution at the trough of the second wave. The calculation results are sensitive to the size of Δx. This is because the non-hydrostatic pressure caused by the curvature of the water surface is important for analysis of the undular jump. Q3D-FEBS can explain the water surface profile of the undular jump up to the second wave by using Δx of about 1/10 of the water depth.

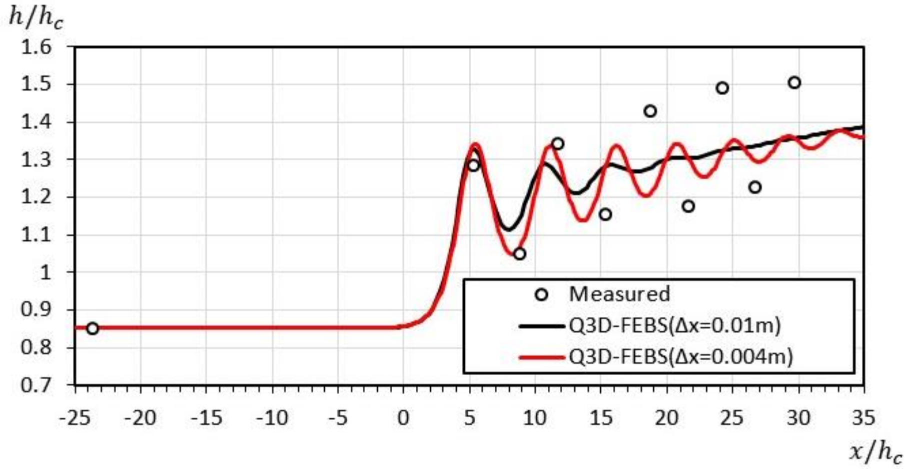

Figure 2. Comparison of measured and calculated water depth profiles of an undular jump.

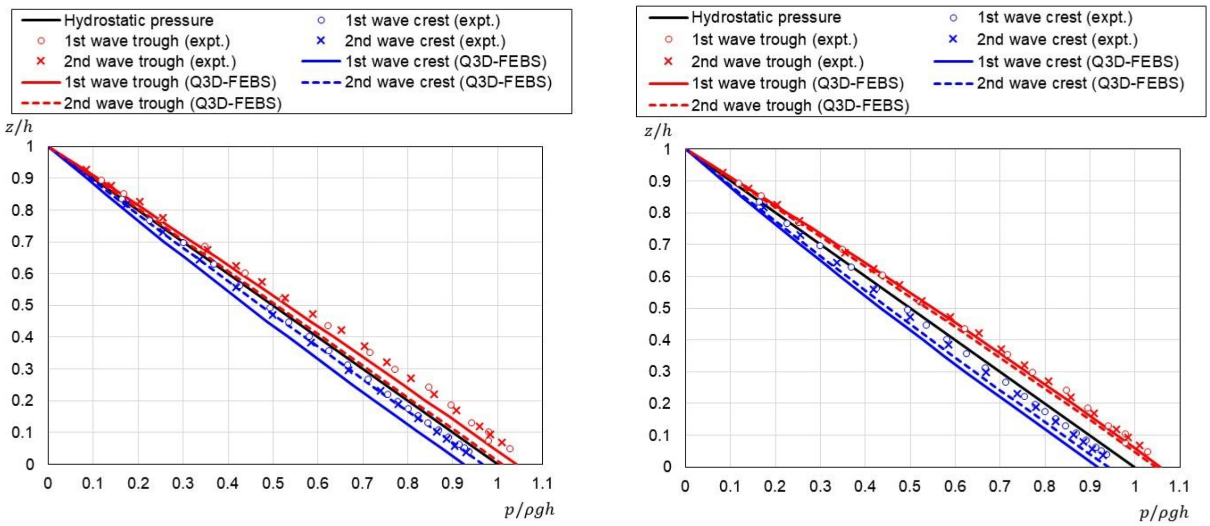

(a) Δx = 0.01 m **(b)** Δx = 0.004 m

Figure 3. Comparison of the vertical distributions of measured and calculated pressure intensity at the crest and trough of the first and second waves of the undular jump.

In the breaking jump experiment (Chacherea & Chanson 2010), the location of the jump was fixed about 1.5 m from the upstream end of the channel. The calculation was performed under the same conditions as the experiment and Δx = 0.02 m ($\Delta x/h_2 \cong 0.12$) was used. Water depths and velocity distributions were measured on the centerline of the channel using acoustic displacement meters and phase-detection conductivity probes. Figure 4 shows the comparison of measured and calculated normalized water depth profiles. The black plots indicate the measured water level averaged over 10 seconds. And the red and blue plots are the measured average water level $\pm$ the standard deviation. The calculation shows only the average water surface profile indicated by the black solid line because the significant fluctuations are not seen in the calculation results. As shown in Figure 4, the water surface profiles calculated by Q3D-FEBS is good agreement with the measured data. Figure 5 is the comparison of measured and calculated velocity distributions. They are averaged over 45 seconds, respectively. The calculation results roughly explain the measured velocity distributions including the backward velocities near the water surface due to the generation of the surface roller. The length of the surface roller estimated from Q3D-FEBS is 0.44m. It is slightly shorter than the length estimated from Eq. [20] (Hager 1999) 0.56 m.

$$\frac{L_r}{h_1} = -12 + 160 \tanh\left(\frac{F_1}{20}\right) \qquad [20]$$

Where, L_r: length of the surface roller, h_1 and F_1: water depth and Fr of approach flow.

From the above results, Q3D-FEBS can well reproduce the water surface profile and velocity distributions of the breaking jump including the generation of the surface roller that is important for estimating the energy dissipation within the jump.

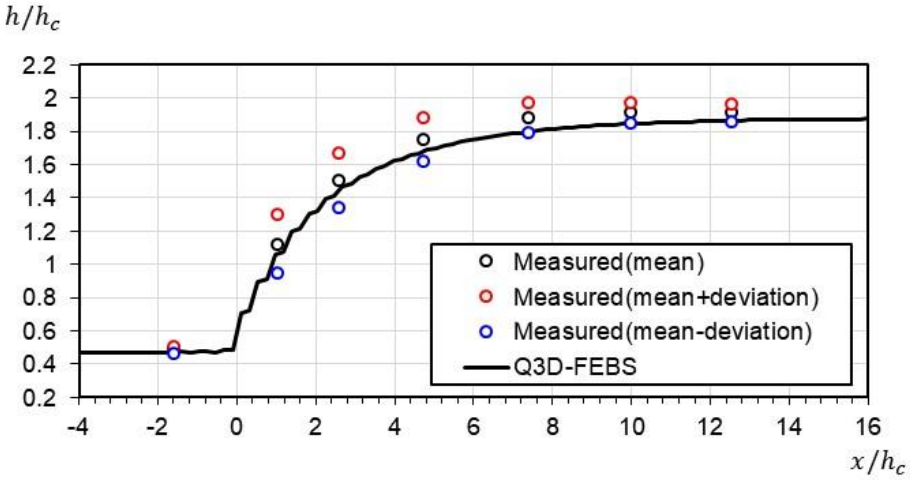

Figure 4. Comparison of measured and calculated water depth profiles of a breaking jump.

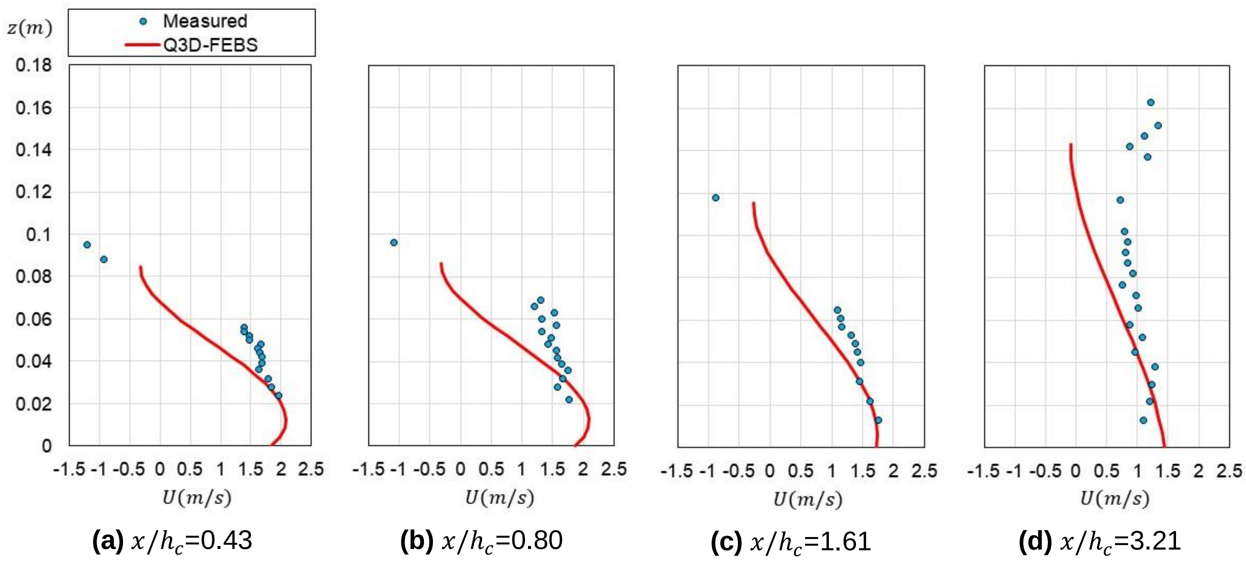

Figure 5. Comparison of measured and calculated velocity distributions of the breaking jump.

4 Numerical simulation of the transitional process from an undular jump to a breaking jump

Using the experimental conditions of Table 1 (Chacherea & Chanson 2010), the transitional process from an undular jump to a breaking jump is simulated by Q3D-FEBS. First, in order to generate an undular jump, a flow rate of 0.02 m^3/s and a water depth of 0.04 m are given at the upstream end and a water depth of 0.054 m is given at the downstream end. After the stable undular jump is formed, Fr of the approach flow grows by increasing the flow rate to 0.0446 m^3/s over 60 seconds while maintaining the water depth at the upstream end at 0.04 m. The water depth at the downstream end is increased to 0.172 m over 55 seconds in order to control the location of the jump. Figure 6 shows the simulation results. As shown in Figure 6(a), (b) and (c), the location of the jump moves downstream and the flow velocities near the water surface are decelerated at the crest of the first wave of the undular jump as Fr increases. When Fr exceeds 2.1, a flow separation occurs at the water surface and it attenuates the wave height as shown in Figure 6(d). After that, the location of the jump moves upstream while expanding the backflow area near the water surface, and finally the breaking jump is formed as shown in Figure 6(e), (f).

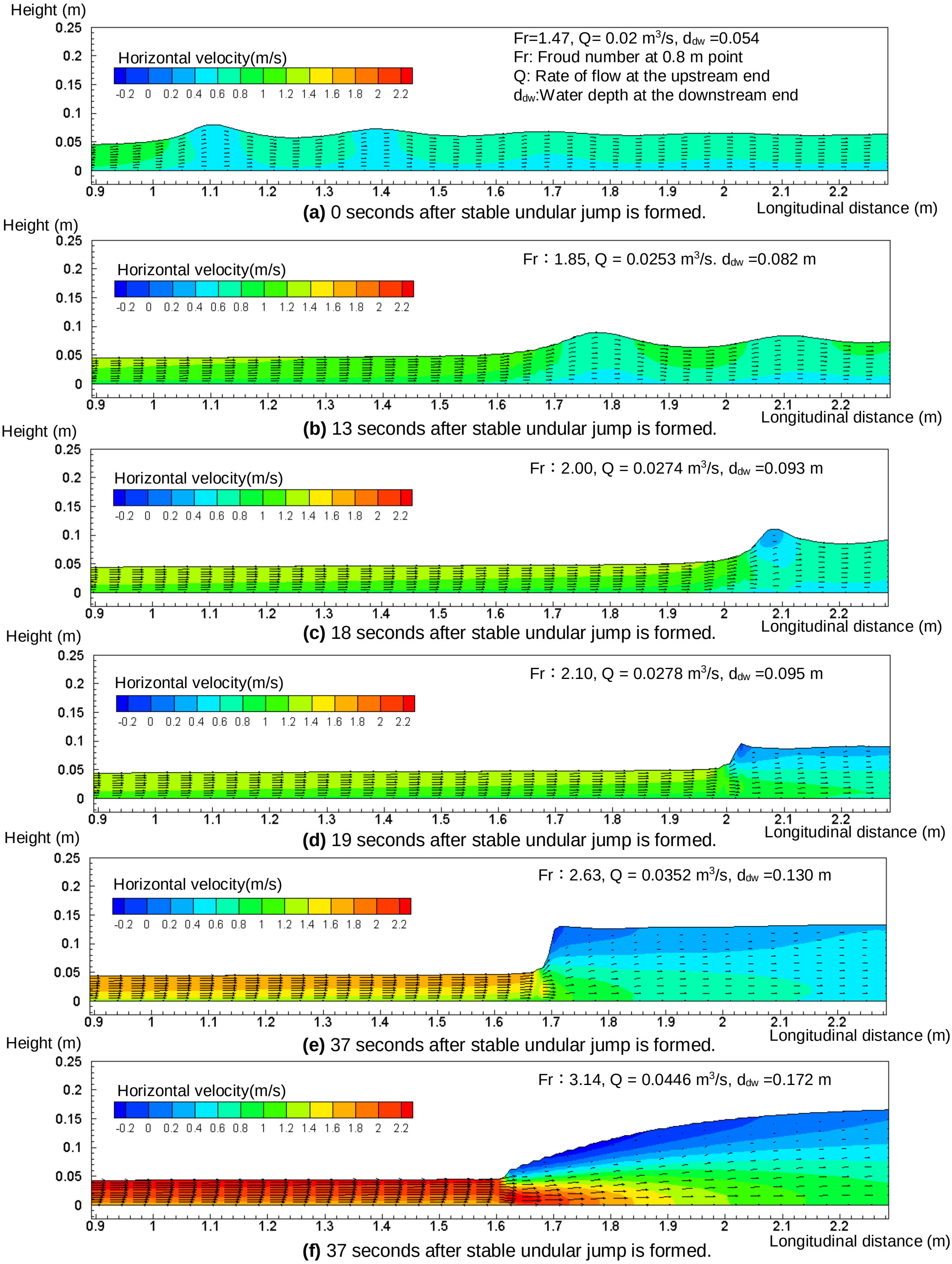

Figure 6. Simulation results of transitional process from an undular jump to a breaking jump by Q3D-FEBS.

It was found that Q3D-FEBS can calculate the transitional process from an undular jump to a breaking jump in the framework of the depth-integral model by analyzing the flow separation at the water surface using the flow equations on boundary surfaces.

5 CONCLUSIONS

This paper proposes a new non-hydrostatic quasi three-dimensional model (Q3D-FEBS) that introduces the flow equations on boundary surfaces (a free surface and a bottom surface). Q3D-FEBS is applied to the previous experiments of undular and breaking jumps and a numerical simulation for the transitional process between the jumps is performed. These results show that Q3D-FEBS can predict the flows in both undular and breaking jumps including the transitional process between the jumps in the framework of the depth-integral model by introducing the flow equations on boundary surfaces.

REFERENCES

Castro-Orgaz, O., Hager, W. H. & Dey, S., (2015). Depth-averaged model for undular hydraulic jump, J*ournal of Hydraulic Research*, 53(3), 351-363.

Chacherea, Y. & Chanson, H., (2010). Free-surface turbulent fluctuations and air-water flow measurements in hydraulics jumps with small inflow Froude numbers, *Report CH78/10*, School of Civil Engineering, The University of Queensland.

Chanson, H., (1993). Characteristics of undular hydraulic jumps, *Research Report CE146*, Department of Civil Engineering, The University of Queensland.

Hager, W. H., (1992). *Energy Dissipators and Hydraulic Jump*, Springer Science & Business Media, 13-18.

Hosoda, T. & Tada, A., (1994). Free surface profile analysis on open channel flow by means of 1-D basic equations with effects of vertical acceleration, *Annual Journal of Hydraulics Engineering*, JSCE, 38, 457-462 (in Japanese).

Iwasa, Y., (1953). Undular jump and its limiting conditions for existence, *Proceedings of the 5th Japan National Congress on Applied Mechanics*, 2(14), 315-319.

Madsen, P. A. & Svendsen, I. A., (1983). Turbulent bores and hydraulic jumps, J*ournal of Fluid Mechanics*, 129, 1-25.

McCorquodale, J. A. & Khalifa, A., (1983). Internal flow in hydraulic jumps, *Journal of Hydraulic Engineering*, 109(5), 684-701.

Narayanan, R., (1975). Wall jet analogy to hydraulic jump, *Journal of the Hydraulics Division*, ASCE, 101(3), 347-359.

Ohno, J., Fukuoka, S., Takemura, Y. & Nigo, S., (2018). Analsis of flood flows in mountain streams with boulders by using non-hydrostatic quasi-three dimensional model (Q3D-FEBS), Proceedings of the 32nd Symposium on Computational Fluid Dynamics, JSFM, C01-1.

Serre, F., (1953). Contribution à l'étude des écoulements permanents et vari-ables dans les canaux, *La Houille Blanche*, 8(12), 830-887 (in French).

Tsubaki, T., (1949). Theory of hydraulic jump, *Reports of the Research Institute for Fluid Engineering*, Kyushu University, Fukuoka, Japan, 5(2), 15-29.

